

Supporting Information for

Polyisobutylene-based glycopolymers as potent inhibitors for *in vitro* insulin aggregation

Asmita Dey,^a Ujjal Haldar,^b Tota Rajasekhar,^b Pooja Ghosh,^a Rudolf Faust,^b and Priyadarsi De^{a,*}

^aPolymer Research Centre and Centre for Advanced Functional Materials, Department of Chemical Sciences, Indian Institute of Science Education and Research Kolkata, Mohanpur 741246, Nadia, West Bengal, India.

^bPolymer Science Program, Department of Chemistry, University of Massachusetts Lowell, One University Avenue, Lowell, Massachusetts 01854, United States.

*Corresponding Author: e-mail: p_de@iiserkol.ac.in

1. Experimental details

1.1. Transmission electron microscopy (TEM) imaging

TEM images were recorded to understand the morphology of **DCP** polymers in aqueous medium, as well as to verify the changes in morphology in fibrillar growth of insulin fibril in the presence of polymeric micelles. Briefly, for analysis of **DCPs** the concentration was fixed at 0.1 mg/mL. Whereas, for insulin fibril and polymer treated insulin fibrils the stock sample set were diluted with 50 mM Tris-HCl buffer (pH 8.0) so that the concentration of each sample was fixed at 50 µg/mL. The samples were drop cased on a carbon-coated 300 mesh TEM grid, air dried and further vacuum dried. Then, TEM images were recorded.

1.2. Field emission scanning electron microscopy (FESEM)

For FESEM analysis, 0.1 mg/mL concentration of each polymer samples were mounted on a cleaned coverslip. For insulin fibril and polymer treated insulin fibrils, 50 µg/mL solutions were drop cased on silicon wafer. The samples were then allowed to dry in air initially, and then placed in a vacuum desiccator. The samples were coated with gold prior to FESEM analysis.

1.3. Dynamic light scattering (DLS) measurements

The size of polymeric aggregates was analysed by DLS measurement using 1 mg/mL solutions. The change in average sizes of insulin fibrils in the absence and presence of polymeric micelles were monitored by DLS measurements. For this experiment, insulin fibril samples were diluted with Milli-Q water to obtain a final concentration of 0.5 mg/mL and then the average sizes were measured.

1.4. Determination of critical aggregation concentration (CAC)

To different concentrations of the block copolymer solutions, a predetermined amount of pyrene in acetone was added and then kept for the acetone to evaporate completely so that the final concentration of pyrene in the solutions is 6.0×10^{-7} mol/L. The solutions were excited at 339 nm wavelength and fluorescence intensities of all the solutions were determined. The ratio of the first and third vibrational peaks from fluorescence intensities for pyrene emission i.e., at 373 nm and 393 nm ($I_3/I_1 = I_{393}/I_{373}$) were plotted *versus* the logarithm of polymer concentration ($\log C$). Two tangent lines were drawn connecting the intensity ratio values from the plot of intensity ratio I_{393}/I_{373} *versus* the $\log C$ and the intersection of these tangents provides the CAC value.¹

1.4. Con A binding study

Addition of glycopolymer solution to the Con A solution results in increased turbidity with time due to aggregate formation.² For the turbidity measurement, 1 mg/mL Con A solution

and 2 mg/mL glycopolymer solution were prepared in phosphate buffer (PBS, pH 7.4). 0.5 mL of Con A solution was taken in the quartz cuvette and absorbance was measured at 420 nm. To the Con A solution, 0.5 mL of glycopolymer solution was added and mixed quickly. The absorbance was monitored immediately from the time of addition till 120 min.

1.5. Circular dichroism (CD) analysis

In order to monitor the changes in secondary structures of insulin fibril in the absence and presence of polymeric micelles, CD technique was employed.³ CD spectra was acquired within 190-240 nm wavelength using 0.1 cm pathlength of cuvette at 25 °C. The bandwidth and response time were set at 1.0 nm and 4 s, respectively, and the scanning speed was maintained at 50 nm/min. Each spectrum was collected three times, and then the average spectra were taken.

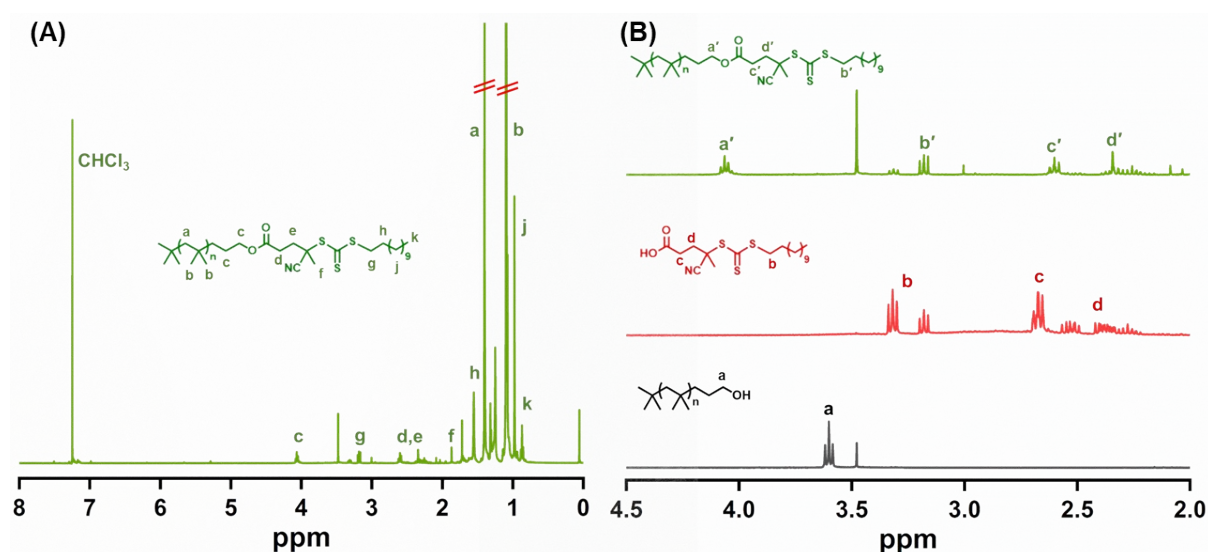


Fig. S1 ¹H NMR spectra of (A) PIB-CDP, and (B) PIB-OH (grey line), CDP (red line) and PIB-CDP (green line) in CDCl₃.

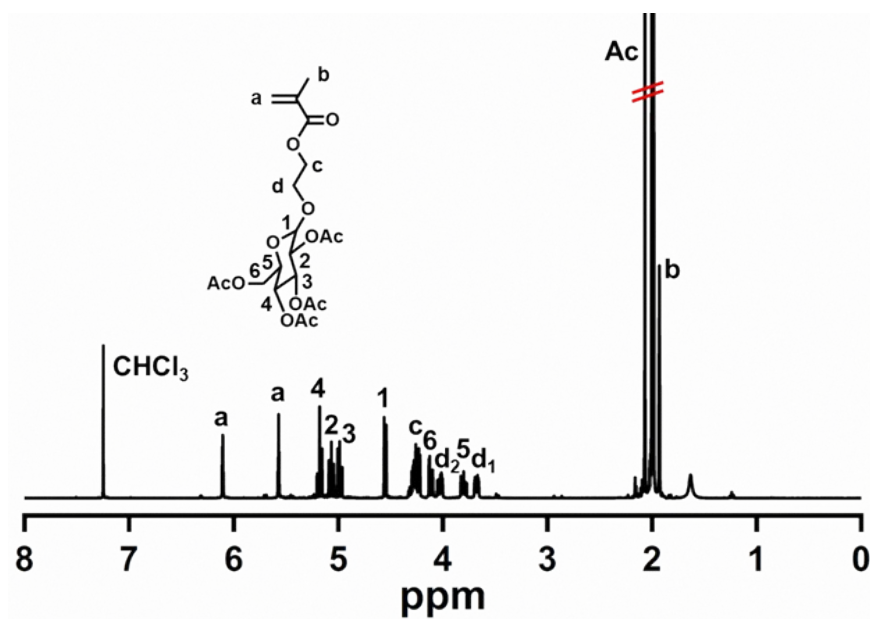


Fig. S2 ^1H NMR spectrum of Ac-G-HEMA in CDCl_3 .

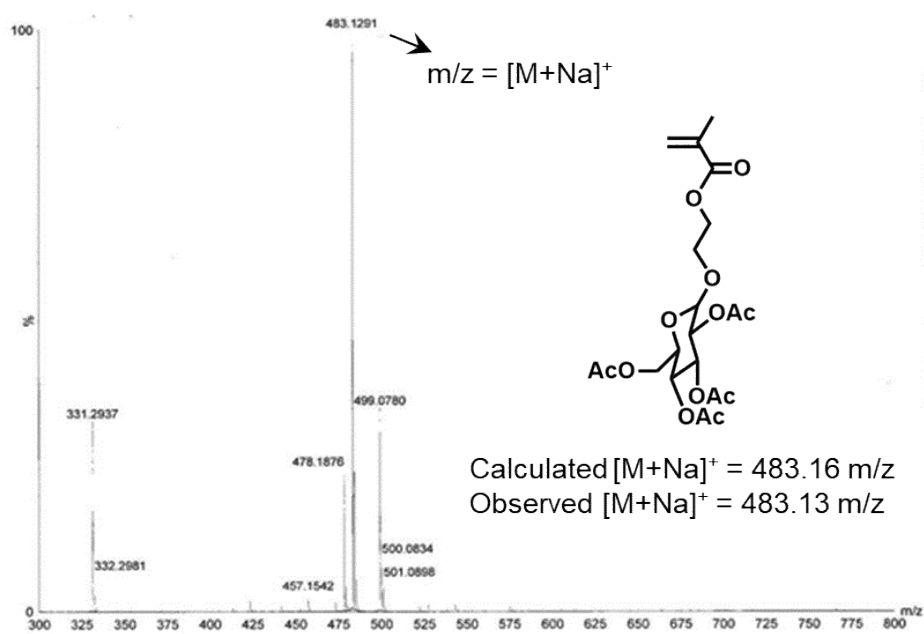


Fig. S3 ESI-MS spectrum of Ac-G-HEMA.

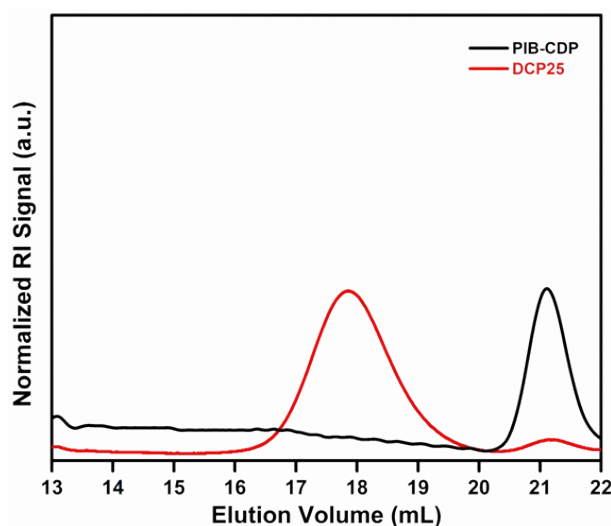


Fig. S4 SEC analysis of **DCP25** in DMF. This measurement was carried out in DMF solvent (flow rate of 0.8 mL/min) at 40 °C. The SEC instrument contains a Waters 1515 HPLC pump, a Waters 2414 refractive index (RI) detector, one PolarGel-M guard column (50 × 7.5 mm), and two PolarGel-M analytical columns (300 × 7.5 mm). The instrument was calibrated by poly(methyl methacrylate) (PMMA) standards from Agilent technologies.

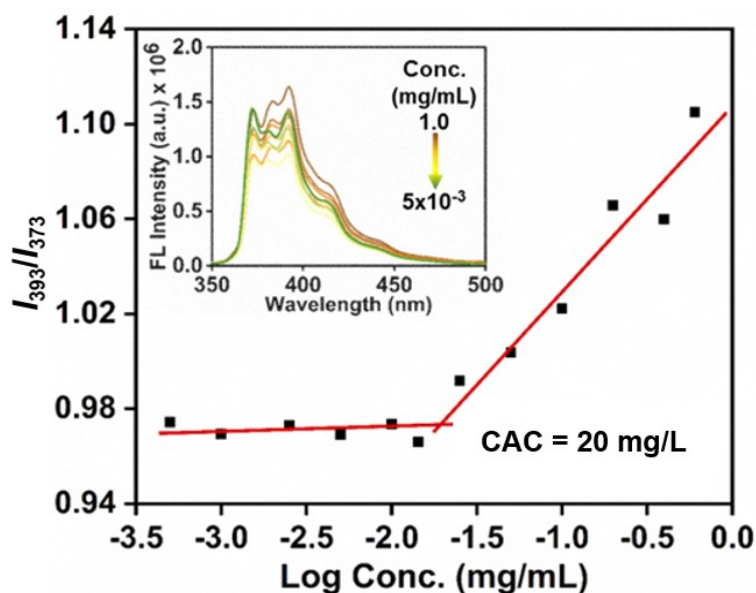


Fig. S5 Determination of CAC for the **DCP25** polymer; the variation in the fluorescence emission spectra of the encapsulated pyrene dye is shown in the inset.

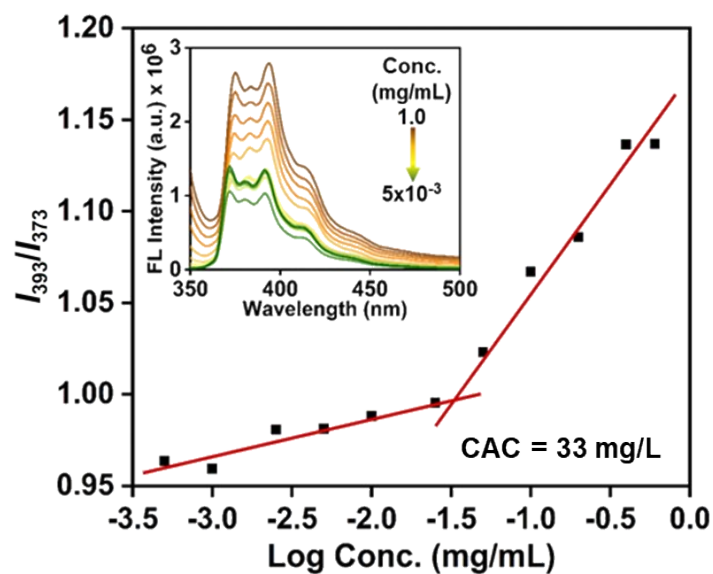


Fig. S6 Determination of CAC for the **DCP60** polymer; the variation in the fluorescence emission spectra of the encapsulated pyrene dye is shown in the inset.

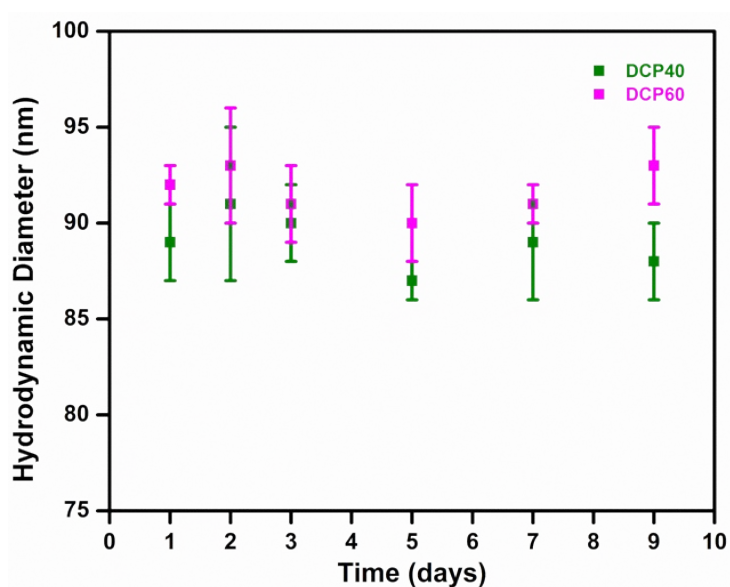


Fig. S7 Stability of **DCP40** and **DCP60** aggregates in water. The polymer solution (1 mg/mL) was stored at 25 °C and hydrodynamic diameter was measured at a regular time interval. The error bar is for the standard deviation.

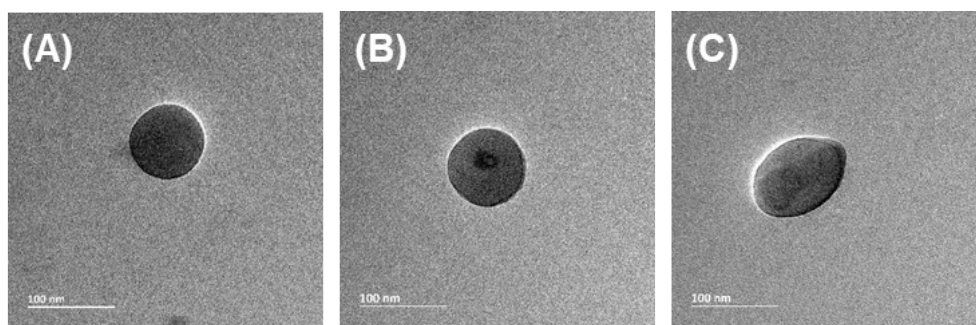


Fig. S8 TEM images of (A) **DCP25**, (B) **DCP40**, and (C) **DCP60** in water.

1.6. Interaction of polymers with lectin protein

Glucose binding helps Con A interact with glycoproteins, which is necessary for Con A's involvement in leukocyte adhesion, tumour metastasis, pathogen recognition, and intercellular communication. Glycopolymers have an enormous advantage over monomeric sugar units due to their multivalent linkage ability with lectin protein i.e., through the glycoside cluster effect.⁴ Factors like structural rigidity, glucose content, polymeric morphology, steric interaction between the glucose units, etc. have a great impact on polymer lectin binding interaction. This aggregate/cluster formation phenomenon between glycopolymers and Con A was monitored using turbidity assay by UV-vis spectroscopy at 420 nm using phosphate buffer solution (Fig. S9A).⁵ The addition of buffer solution of polymers to 1 mg/L buffer solution of Con A resulted in the formation of a precipitate, thus the turbidity of the solution increased (Fig. S10). The higher the glucose content the greater should be the interaction and binding, thus steeper slope was expected in the absorption *versus* reaction time plot. For the **DHP50** homopolymer, the slope was much steeper compared to that in the case of block copolymers (**DCPs**). This states that the homopolymer has a better ability to bind with lectin; this is because in **DHP50** all the glucose units were exposed to the solution and they do not have a steric hindrance factor. But in case of **DCPs**,

they formed micellar morphology in water, thus glucose units came close to each other to decrease the spacing between them as a result steric factor plays an important role. Therefore, it became easier for the Con A to bind faster to homopolymer rather than in block copolymers (Fig. S9A). Again, on increasing the glucose content within the polymer in case of **DCPs** the slope becomes steeper. This is because as the number of glucose units increased the number of interacting units also increased, thus better binding was observed.

Binding interactions of the polymers with Con A were measured by ITC, which provided the magnitude of binding affinity, and the two important thermodynamic parameters: enthalpy (ΔH) and entropy (ΔS) changes.⁶ Fig. S9B represents a calorimetric titration profile for the binding of **DCP60** to Con A at 25 °C. In the inset of Fig. S9B, each peak represents a single injection of the polymer into the Con A protein solution. An integrated plot of the amount of heat liberated per injection as a function of the molar ratio of the polymer to protein has been represented in Fig. S9B. The ΔH and $T\Delta S$ showed -80.0 kcal/mol and -74.3 kcal/mol values for interaction of Con A with **DCP60**. The $\Delta H < 0$, and $\Delta S < 0$ imply that the interaction was exothermic and polar interaction played a major role.

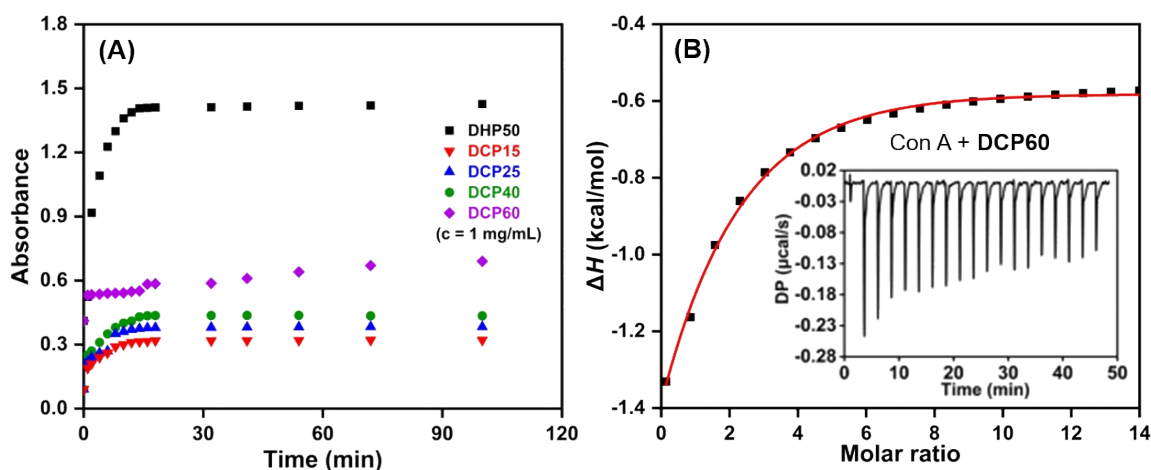


Fig. S9 (A) Con A binding turbidimetry assay experiment with **DHP50** and **DCPs** at $\lambda_{\text{ex}} = 420$ nm. (B) ITC profiles of Con A in the presence of **DCP60**.

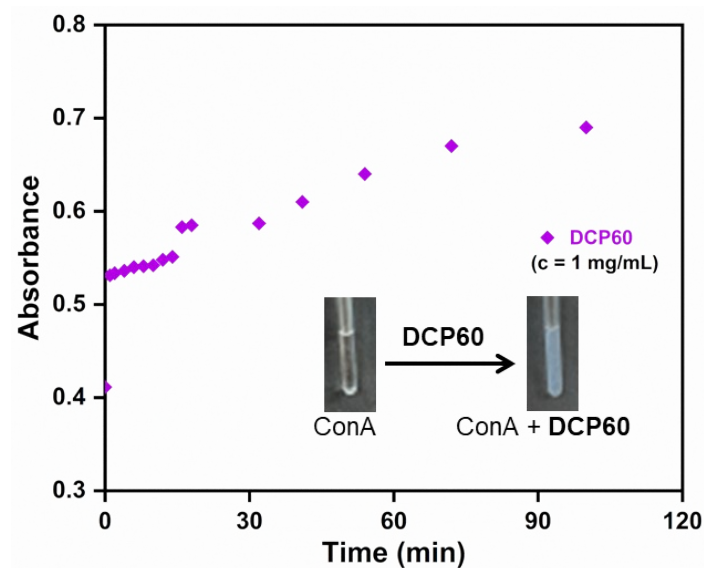


Fig. S10 Con A binding turbidimetry assay experiment with **DCP60**. Turbidity appears on addition of buffer solution of **DCP60** to 1 mg/mL buffer solution of Con A. Other polymers **DHP50**, **DCP15**, **DCP25**, and **DCP40** showed similar turbidity effect on Con A binding turbidimetry experiment.

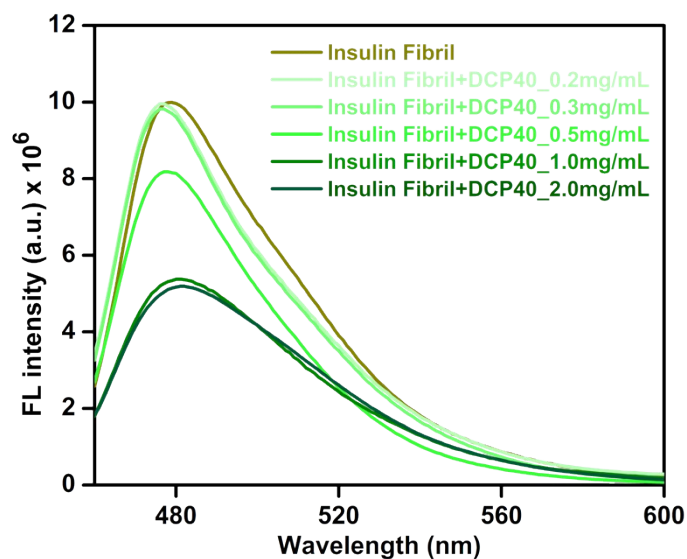


Fig. S11 ThT fluorescence spectra of insulin fibrils before and after treatment with different concentrations of **DCP40**.

Table S1 %Inhibition rate of insulin fibrillation on treatment with different polymers.

| Sample | Inhibitory rate (%) |
|--------------|---------------------|
| DHP50 | 14 |
| DCP15 | 45 |
| DCP25 | 65 |
| DCP40 | 72 |
| DCP60 | 77 |

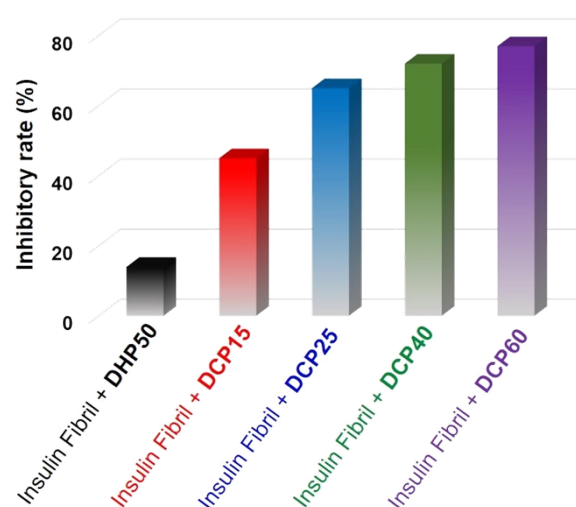


Fig. S12 Histogram of the %inhibition rate of insulin fibrillation on treatment with different polymers.

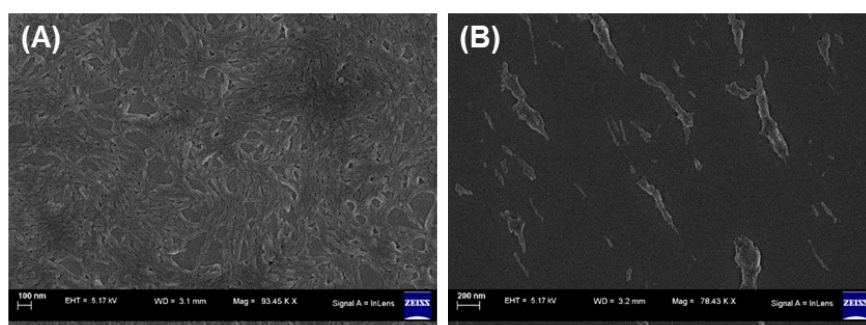


Fig. S13 FESEM images of insulin fibrils in the absence of polymer (A), and in the presence of **DCP60** (B).

References

- 1 K. Kalyanasundaram and J. K. Thomas, *J. Am. Chem. Soc.*, 1977, **99**, 2039-2044.
- 2 A. P. P. Kröger, M. I. Komil, N. M. Hamelmann, A. Juan, M. H. Stenzel and J. M. J. Paulusse, *ACS Macro Lett.*, 2019, **8**, 95-101.
- 3 V. P. Mahendra, K. Y. Prasad, P. Ganesan and R. Kumar, *Mol. Biol. Rep.*, 2020, **47**, 2811-2820.
- 4 C. Müller, G. Despras and T. K. Lindhorst, *Chem. Soc. Rev.*, 2016, **45**, 3275-3302.
- 5 T. J. Paul, A. K. Strzelczyk, M. I. Feldhof and S. Schmidt, *Biomacromolecules*, 2020, **21**, 2913-2921.
- 6 D. Prozeller, S. Morsbach and K. Landfester, *Nanoscale*, 2019, **11**, 19265-19273.